Ann. Limnol. - Int. J. Lim. 51 (2015) 23–35
© EDP Sciences, 2015
DOI: 10.1051/limn/2014031

Available online at:
www.limnology-journal.org

Estimating sediment and particulate organic nitrogen and particulate organic phosphorous yields from a volcanic watershed characterized by forest and agriculture using SWAT model

Chunying Wang[1]*, Rui Jiang[2], Xiaomin Mao[3], Sabine Sauvage[4,5], José-Miguel Sánchez-Pérez[4,5], Krishna P. Woli[6], Kanta Kuramochi[1], Atsushi Hayakawa[7] and Ryusuke Hatano[1]

[1] Graduate School of Agriculture, Hokkaido University, 0600808 Sapporo, Japan
[2] College of Resources and Environment, Northwest A&F University, 712100 Yangling, China
[3] Center for Agricultural Water Research in China, China Agricultural University, 100083 Beijing, China
[4] Laboratoire Ecologie Fonctionnelle et Environnement (EcoLab), University of Toulouse, INPT, UPS, Avenue de l'Agrobiopole, 31326 Castanet Tolosan Cedex, France
[5] CNRS, EcoLab, 31326 Castanet Tolosan Cedex, France
[6] Department of Agronomy, Iowa State University, 1318 Ames, USA
[7] Akita Prefectural University, 0100195 Akita, Japan

Received 20 March 2014; Accepted 13 July 2014

Abstract – The study was conducted in the Shibetsu River watershed (SRW), Hokkaido, Japan, in order to examine the possibility of using the soil and water assessment tool (SWAT) to provide an understanding of sediment and particulate organic nitrogen (PON) and particulate organic phosphorous (POP) yields between 2003 and 2008. The SRW is a non-conservative catchment (the surface catchment lying on a continuous impervious horizon) and it is recognized that it receives external groundwater (EXT) from other watersheds. The EXT yield from each hydrologic response unit (HRU) was added to streamflow in the SWAT model. Simulated daily sediment and PON and POP yields from the SWAT model showed a strong agreement with the observed values. The simulated annual sediment yield ranged from 5 to 45 tonnes.km^{-2}.yr^{-1} (annual mean of 24 tonnes.km^{-2}.yr^{-1}). Annual PON yield ranged from 0.1 to 0.3 tonnes.km^{-2}.yr^{-1} (annual mean of 0.18 tonnes.km^{-2}.yr^{-1}). Annual POP yield ranged from 0.01 to 0.03 tonnes.km^{-2}.yr^{-1} (annual mean of 0.02 tonnes.km^{-2}.yr^{-1}). Snowfall, snowmelt and rainfall seasons contributed about 10, 20 and 70% respectively to total sediment and associated PON and POP yields. The SWAT model identified that sub-basins located in the upper part of the watershed were critical source area of land surface erosion. This research demonstrates the ability of the SWAT model to estimate sediment and associated PON and POP yields, and to improve the understanding of soil erosion mechanisms at catchment scale receiving external water.

Key words: Particulate organic nitrogen (PON) / particulate organic phosphorous (POP) / sediment yield / soil and water assessment tool (SWAT)

Introduction

Sediment and sediment-bound pollutants, including pesticides, particulate nutrients, heavy metals and other toxic substances transported from the land surface to stream networks are responsible for reservoir sedimentation and aquatic habitat degradation (Haag *et al.*, 2001; Boithias *et al.*, 2011, 2013; Kerr *et al.*, 2011; Cerro *et al.*, 2013, 2014). Several adverse economic and environmental impacts due to the damaging effects of soil erosion have been reported. The on-site effect of soil erosion in terms of declining soil fertility and decreased agricultural yields are well known around the world. Environmental consequences are primarily off-site effects due to the pollution of natural waters (Lal, 1998). Understanding the dynamics of sediment transfer from land to watercourses and quantifying sediment yields are essential for controlling land soil erosion and implementing appropriate mitigation practices to reduce stream sediment and associated pollutant loads, and hence improve surface

*Corresponding author: wangchunying1987@yahoo.com

water quality downstream (Heathwaite *et al.*, 2005). Downstream erosion and sedimentation implications are of increasing interest for catchment management, such as the design of dam reservoirs, river restoration, the design of stable channels and the protection of fish and wildlife habitat.

It has remained a challenge to estimate changes in sediment yield over time in a catchment owing to the complexity of the processes involved in the detachment and transport of fluvial sediment. Different approaches have been adopted for sediment yield estimation. The most reliable method for sediment load estimation is direct measurement at the catchment level. Sediment concentrations are usually measured infrequently because very frequent monitoring over the long term is costly. It has also been noted that a sediment sampling strategy should be designed to capture high sediment concentrations for long-term monitoring to provide better results (Thomas, 1988).

The applications of empirical models for estimating sediment load have shown promise. Estimation of sediment load is commonly achieved by establishing a sediment rating curve. Empirical rating curves describing relationships between sediment load and instantaneous water discharge are often used. Some researchers have suggested that an excellent sediment rating curve could be constructed using a limited set of data (Gao, 2008). Sediment rating curves are useful in predicting sediment yield, but they are site specific and have limitations when it comes to interpreting erosion processes (landscape erosion and in-stream erosion/sedimentation). Distributed and process-based watershed models are capable of capturing these complex processes both spatially and temporally. This category of models can be used to provide an enhanced understanding of the relationship between hydrologic processes, landforms, land management, soil factors and erosion/sedimentation (Van Rompaey *et al.*, 2001; Easton *et al.*, 2010). Many of the model parameters have a physical meaning and can be measured in the field, and therefore model validation can be concluded on the basis of a short field survey and a short time series of meteorological and hydrological data. Various hydrological models have been proposed to predict sediment export to rivers, such as the European soil erosion model (EUROSEM) (Morgan *et al.*, 1998), the water erosion prediction project (WEPP) (Nearing *et al.*, 1989) and the soil and water assessment tool (SWAT) (Neitsch *et al.*, 2005).

The sediment yield estimation model used in this study is the SWAT model. It is a comprehensive process-based model that simulates water, sediment and chemical fluxes in watersheds under varying climatic conditions, soil properties, stream channel characteristics, land use and agricultural management (Jayakrishnan *et al.*, 2005; Talebizadeh *et al.*, 2010). The SWAT model has been applied to enhance understanding of sediment loss and transport processes over a wide range of environments around the world (Oeurng *et al.*, 2011). For sediment yield modelling, Mukundan *et al.* (2010) examined the suitability of SWAT at the North Fork Broad River catchment located in the Piedmont region of Georgia, and their results suggested that the SWAT model is a better substitute than the sediment rating curve for estimating sediment yield. Many researchers have reported that the SWAT model predicted reasonable results for sediment yield estimation (especially on monthly and yearly timescales) when provided accurate input data and model parameterization (Chu *et al.*, 2004; Saghafian *et al.*, 2012).

The SWAT model can estimate soil erosion from the landscape and in-stream depositional and degrading processes. The sediment yield from the landscape is calculated using the modified universal soil loss equation (MUSLE; Williams, 1975). Sediment deposition and degradation in the stream channel are both calculated during sediment routing. The maximum amount of sediment that can be transported from a reach segment during the channel sediment routing is determined by the modified Bagnold's equation (Bagnold, 1977). However, both MUSLE and the modified Bagnold's equation in the SWAT model are empirical equations; therefore SWAT may not produce accurate results in all situations. As a surface hydrological model, SWAT also has limited applicability in complex hydrological environments, such as non-conservative watersheds where the drainage area does not correspond to the hydrological watershed. Non-conservative watersheds may either lose internal groundwater to neighbouring watersheds or gain external groundwater (EXT) originating from outside the watershed. These inter-catchment groundwater fluxes are made possible by the well-known karstification phenomena, widespread in limestone all over the world, although similar phenomena can also exist in volcanic substrata as well as in chalk horizons (Le Moine *et al.*, 2008; Jiang *et al.*, 2011). The evaluation of the hydrological component of SWAT completed in previous studies has pointed out that SWAT has no mechanism to account for external water (EXT) contributions through subsurface flow from outside the watershed (Chu *et al.*, 2004; Salerno and Tartari, 2009). Consequently, the SWAT model cannot consider the effect of EXT on sediment routing in reaches where EXT finally enters. Jiang *et al.* (2011, 2014) examined the possibility of using the SWAT model in a non-conservative watershed, the Shibetsu River watershed (SRW, 672 km^2, Hokkaido, Japan), which is recognized to receive external groundwater. They reported that the SWAT model could be successfully used to understand components of stream discharge and nitrate export by assuming EXT as a constant value (1.38 $mm.d^{-1}$, estimated from a long-term annual water balance budget) and including it as a point source of water and nitrate in the model. However, the suitability of the SWAT model for estimating sediment and associated particulate organic nitrogen (PON) and particulate organic phosphorous (POP) yields and for understanding the soil erosion mechanism by taking into account the EXT contribution to streams is still unclear in the Shibetsu River watershed.

The main objective of this study was to apply the SWAT model to accurately estimate sediment and

associated PON and POP yields and to understand soil erosion mechanisms in SRW containing forest and agriculture, which is dominated by volcanic soils with an EXT source.

Materials and methods

Study site description

The SRW is located in Eastern Hokkaido, Japan (Fig. 1). This region has a hemi-boreal climate with long-term (1980–2008) average annual precipitation of 1128 mm and an annual mean temperature of 5 °C (Japan Meteorological Agency, http://www.jma.go.jp). The weather stations and main outlet locations are shown in Figure 1.

The SRW is characterized as receiving a large amount of external water from neighbouring watersheds, although there are no external surface rivers, streams or ditches from neighbouring watersheds flowing into the SRW. However, the presence of springs and volcanic substrata in this watershed indicates that the geology presents a comprehensive picture of a rich underground water network, with external water recharging the SRW as groundwater (Le Moine *et al.*, 2007; Jiang *et al.*, 2011). About 29% of the watershed is a mountainous area where slopes are greater than 10% and elevations range from 295 to 1059 m, as shown in Fig. 1 (Jiang *et al.*, 2011). The SRW was divided into sub-basins based on the stream network (Fig. 1). The major soil types of the SRW include Peat soils (3.26%), Regosolic Kuroboku soils (13.94%), Brown Forest soils (20.56%), Kuroboku soils (46.08%), Brown Lowland soils (9.10%), Regosols (4.51%) and Grey Lowland soils (2.55%) (Cultivated Soil Classification committee, Japan, 1995), which corresponds to Histosols, Vitric Andosols, Cambisols, Silandic Andosols, Haplic Fluvisols, Regosols and Gleyic Fluvisols, in the World Reference Base (WRB), respectively (IUSS, 2006). The principal characteristics of the soils have been presented by Jiang *et al.* (2011). All the soils in this watershed are volcanogeneous soils. Land uses of the SRW consist of forest (53.7%), agriculture (40.8%), urban (4.5%) and water (1.0%). Pastureland occupies more than 95% of the agricultural land area and the remaining minor agricultural crops are ignored in this study. The SRW soil and land use maps are shown in Figure 1. Substantial sediment may enter stream water through surface runoff due to steep slopes in the mountainous area or improper intensive dairy farming in the pastureland (Woli *et al.*, 2004; Hayakawa *et al.*, 2009; Jiang *et al.*, 2011).

Instrumentation and sampling

For the whole watershed outlet of the SRW, hourly stream discharge data (2003–2008) were obtained from the Water Information System (Ministry of Land, Infrastructure and Transport, Japan).

Water samples were collected using an autosampler (ISCO℠ 3700, Isco, Lincoln, NE, USA). The autosampler was triggered when rainfall was >4 mm per 30 min, with sampling intervals of 15 min to 1 h for the rising stage of discharge and 2–6 h for the receding stage. This sampling method generated a high sampling frequency during storm events. After sampling, the water samples were stored on ice until transportation to the laboratory where they were then stored at 4 °C until analysis. Water samples were filtered through 0.7 μm glass microfibre filters for the analysis of suspended sediments. A portion of the water samples were filtered through 0.2 μm membrane filters within a few days, and analysed for total dissolved nitrogen (TDN) and total dissolved phosphorous (TDP). The remaining non-filtered samples were used for total nitrogen (TN) and total phosphorous (TP) analysis. Concentrations of TN, TP, TDN and TDP were determined using the method of alkaline persulphate digestion and HCl-acidified UV detection. The PON and POP concentrations were calculated by subtracting the concentration of TDN from TN and TDP from TP, respectively (Hayakawa *et al.*, 2009). Sediment and PON and POP yields were calculated from the sediment concentrations and discharge data.

Model description and model input

The SWAT model is a spatially distributed, physically process-based model for predicting the movement of water, sediment and chemicals in complex catchments with varying soils, land uses and management conditions over long periods of time. Major model components include weather, hydrology, soil temperature and properties, plant growth, nutrients, pesticides, bacteria and pathogens, and land management. The SWAT model simulates water and nutrient cycles within numerous sub-basins, which are then further subdivided into hydrologic response units (HRUs) that consist of homogeneous land use, soil and terrain characteristics. These steps resulted in 278 individual HRUs within the 77 sub-basins in the Shibetsu River watershed.

In a conservative environment, the total water entering channels every day from each HRU in the SWAT model can be derived from

$$Q_{\text{flow}} = (q_{\text{surf}} + q_{\text{lat}} + q_{\text{gw}}) \times \text{HRU}_{\text{area}} \quad (1)$$

where Q_{flow} is the total water entering the channel of the sub-basin where the HRU is located (mm^3), q_{surf} is surface runoff yield (mm), q_{lat} is lateral flow yield (mm), q_{gw} is groundwater yield (mm) and HRU_{area} is the HRU area (mm^2).

For the non-conservative environment, in this study the EXT flow into the sub-basin channel from each HRU was added to the total water entering the channels in the SWAT model, which can be described by

$$Q_{\text{flow}} = (q_{\text{surf}} + q_{\text{lat}} + q_{\text{gw}} + \text{EXT}) \times \text{HRU}_{\text{area}} \quad (2)$$

where q_{gw} here is the internal groundwater yield (mm) and EXT is the external groundwater yield from outside the

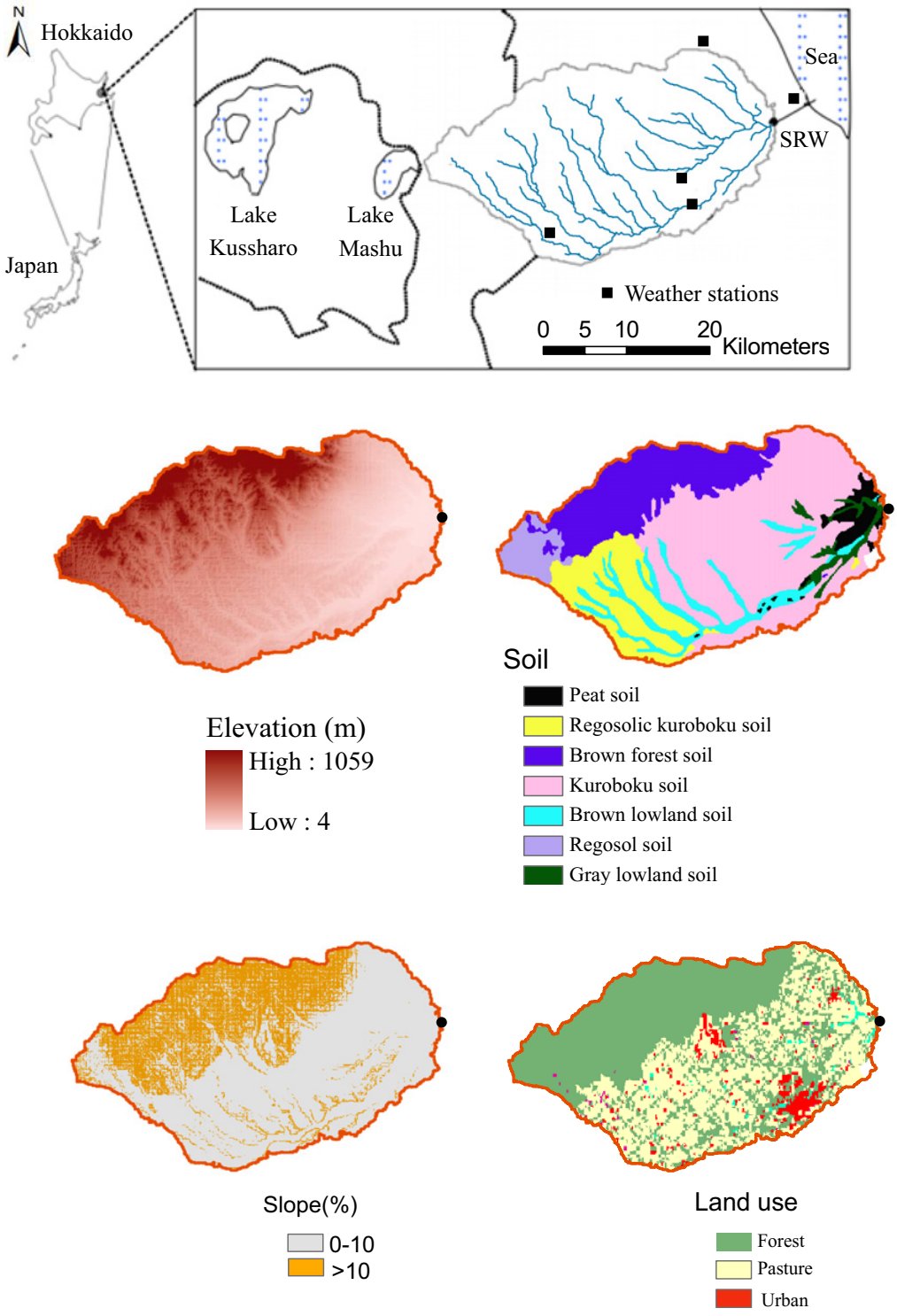

Fig. 1. Locations of weather stations and sampling sites, sub-basins, stream network, digital elevation model (DEM), slope, land use and soil maps.

watershed (mm). For simplification, EXT was added as 1.38 $mm.d^{-1}$ without temporal and spatial variations in this study. This value was calculated from the annual water balance budget from 1980 to 2008 (Jiang *et al.*, 2011). Note that EXT actually varies both temporally and spatially. Hence, EXT added as a constant yield in SWAT should be treated with caution if the dynamics of EXT are significant.

The SWAT model estimates soil erosion and sediment yield from the landscape and in-stream depositional and degrading processes. The sediment yield from the landscape is calculated using the MUSLE (Williams, 1975).

Table 1. Parameters for streamflow calibration performed at the Shibetsu River watershed.

No	Parameters	Definition of parameters	Fitted value
1	CN2.mgt	Initial SCS runoff curve number for moisture condition II	Forest (36) Pasture (45) Urban (55)
2	ALPHA_BF.gw	Baseflow alpha factor (days)	Forest (0.02) Pasture (0.5) Urban (0.5)
3	REVAPMN.gw	Threshold depth of water in the shallow aquifer for revap to occur (mm)	210
4	SOL_AWC.sol (all soil layers)	Available water capacity of the soil layer (mm H_2O mm.soil^{-1})	0.10
5	ESCO.hru	Soil evaporation compensation factor	0.29
6	CANMX.hru	Maximum canopy storage (mm H_2O)	39
7	GW_DELAY.gw	Groundwater delay (days)	Forest (3) Pasture (0.5) Urban (0.5)
8	CH_N2.rte	Manning's "*n*" value for the tributary channels	0.09
9	SFTMP.bsn	Snowfall temperature (°C)	1.9
10	SMTMP.bsn	Snowmelt base temperature (°C)	1.6
11	SMFMX.bsn	Maximum melt rate for snow during years (mm. °C^{-1}.d^{-1})	1.2
12	SMFMN.bsn	Minimum melt rate for snow during years (mm. °C^{-1}.d^{-1})	0.2
13	TIMP.bsn	Snowpack temperature lag factor	0.6
14	SURLAG.bsn	Surface runoff lag coefficient	0.9

Sediment deposition and degradation in the stream channel are both calculated during the sediment routing. The channel sediment routing equation uses a modification of Bagnold's sediment transport equation (Bagnold, 1977). Whether channel deposition or channel degradation occurs depends on the sediment load entering the channel and the maximum amount of sediment that can be transported in the channel. EXT has no effect on surface erosion processes because it enters the channel as groundwater; therefore, EXT does not contain any input of sediment and particulate nutrients to the stream. However, because EXT increased the total water amount in channels, it can cause dilution of sediment, PON and POP present in the stream. Also it may increase the maximum amount of sediment that can be transported in the channel.

In this study, the inputs required by the model are daily weather data for precipitation, maximum and minimum temperature, wind speed, solar radiation and relative humidity, which were obtained from the weather stations' records (Fig. 1) from 1997 to 2008. Digital elevation model (DEM) data (Fig. 1) was prepared using a digital map with a 30 m grid elevation created from a 1:25 000 topographic map published by the Japanese Geographical Survey Institute (GSI, http://nlftp.mlit.go.jp/ksj/jpgis/jpgis_datalist.html). GIS-referenced soil data (Fig. 1) were extracted from a 1:50 000 soil map of the Fundamental Land Classification Survey developed by the Hokkaido Regional Development Bureau (www.agri.hro.or.jp/chuo/kankyou/soilmap/html/map_index.htm). A land use map (1:25 000) based on land cover in 2005 was obtained from the GSI (Fig. 1). Weather data, land use classification, soil types and the major soil characteristics have been published by Jiang *et al.* (2011).

The SWAT model with EXT was used to estimate sediment yield at the main outlet of SRW. Then, based on the estimated sediment yield and its relationships with PON and POP yields, PON and POP yields were estimated further. The SWAT results were investigated and compared with the observed values to evaluate its performance for estimating sediment and PON and POP yields in the SRW.

Model calibration and validation

The SWAT model was first calibrated using SWAT Calibration and Uncertainty Programs (CUP) with the Sequential Uncertainty Fitting (SUFI2) calibration and uncertainty analysis routine (Abbaspour, 2007). Then the calibration of flow and sediment was performed manually to obtain a good match between the observed and simulated values. Key hydrological and sediment-related parameters were selected, based on suggestions from Jiang *et al.* (2011) and Phomcha *et al.* (2011). Calibration is an effort to better parameterize a model to a given set of local conditions, thereby reducing the prediction uncertainty. Model calibration is performed by carefully selecting values for model input parameters by comparing model predictions for a given set of conditions with observed data for the same conditions. Model validation is the process of demonstrating that a given site-specific model is capable of making sufficiently accurate simulations. Validation involves running a model using parameters that were determined during the calibration process, and comparing the predictions to observed data not used in the calibration. Calibration and validation are typically performed by splitting the available observed data into two datasets: one for calibration, and another for validation. Data are most frequently split by time periods (Arnold *et al.*, 2012). In this study, parameters calibrated for streamflow are shown in Table 1. In the study site, previous study by Jiang *et al.* (2011) showed that the streamflow increased at the same day as rainfall happened, which indicated that the response of streamflow to surface

Table 2. Soil saturated hydraulic conductivity (K) and USLE soil erodibility (K_{USLE}) factor.

Soil type	K (mm.h^{-1})	K_{USLE}
Peat soil	59	0.24
Regosolic kuroboku soil	123	0.23
Brown forest soil	46	0.18
Brown lowland soil	122	0.23
Regosol soil	151	0.19
Grey lowland soil	75	0.25
Kuroboku soil	114	0.22

runoff is very quick. Therefore, the value of SURLAG was adjusted within one day. Other parameters were also calibrated within their acceptable ranges to match the simulated streamflow with the observed streamflow (Table 1). The streamflow was calibrated from 2003 to 2005 and validated from 2006 to 2008. The SWAT model was further used for sediment yield calibration following completion of the streamflow calibration process. The USLE soil erodibility factor (K_{USLE}) was calculated from an equation proposed by Williams (1995) based on clay, silt, sand and organic carbon contents in soil (Table 2). The USLE topographic factor (LS_{USLE}) based on SLSUBBSN.hru and HRU_SLP.hru was automatically calculated from the GIS interface in the SWAT model. The EXT contribution increased the stream water yield (Jiang *et al.*, 2011) and it can dilute the sediment concentration significantly. Consequently, it can increase sediment transport capacity in channels, sediment deposition in the channels might not happen. Therefore, the maximum values of SPCON (0.01) and SPEXP (2) were used to reduce deposition in the channel. Other model parameters were calibrated within their acceptable ranges to match the simulated sediment loadings with the observed loadings (Table 3). Observed sediment loads were used to calibrate SWAT in 2003 and the model was validated in 2004. The study period for sediment was only 2 years (2003–2004) because most samples were collected in these 2 years. Note that the calibration and validation periods were short due to the lack of long-term observed data. Longer calibration and validation periods would provide more confidence in the model parameters.

Model performance evaluation

The accuracy of SWAT simulation results was determined by examining the coefficient of determination (R^2), the Nash and Sutcliffe (1970) efficiency (E_{NS}) and relative error (Re). The R^2 value is an indicator of the strength of the linear relationship between the observed and simulated values. The E_{NS} simulation coefficient indicates how well the plot of observed values versus simulated values fits the 1:1 line. If the R^2 and E_{NS} values are less than or very close to zero, the model prediction is unacceptable or poor. If the values are one, then the model prediction is perfect (Santhi *et al.*, 2001). Re also indicates how close the observed values versus the simulated values are. Re can range from zero to a very large value, with zero representing perfect agreement between the model and real data. Essentially, when the model efficiency R^2 and E_{NS} are close to one, and when the model efficiency Re is close to zero, the models are considered more accurate.

R^2 is statistically defined as

$$R^2 = \left\{ \frac{\sum_{i=1}^{n} \left(X_{oi} - \overline{X_{oi}}\right)\left(X_{si} - \overline{X_{si}}\right)}{\left[\sum_{i=1}^{n} \left(X_{oi} - \overline{X_{oi}}\right)^2\right]^{0.5} \left[\sum_{i=1}^{n} \left(X_{si} - \overline{X_{si}}\right)^2\right]^{0.5}} \right\} \quad (3)$$

E_{NS} is statistically defined as

$$E_{NS} = 1 - \frac{\sum_{i=1}^{n} \left(X_{oi} - X_{si}\right)^2}{\sum_{i=1}^{n} \left(X_{oi} - \overline{X_{oi}}\right)^2} \quad (4)$$

Re (in percentage) at the gauge locations can be derived from

$$\mathrm{Re}(\%) = \left| \frac{\sum_{i=1}^{n} X_{si} - \sum_{i=1}^{n} X_{oi}}{\sum_{i=1}^{n} X_{oi}} \right| \times 100 \quad (5)$$

where X_{oi} is the observed data on day i, X_{si} is the simulated output on day i, $\overline{X_{oi}}$ is the average measured value during the study period, and n is the total number of the observed data.

Results and discussion

PON and POP

The partition of dissolved and particulate nitrogen and phosphorous is shown in Table 4. PON accounted for 4, 23 and 32% of TN during snowfall (December to March), snowmelt (April to May) and rainfall (June to November) seasons, respectively. PON partitioned only 4% of the TN during the snowfall season, but its partition increased to 23% during the snowmelt season and to 32% during the rainfall season. POP is the main form of phosphorous, which accounted for 92% of TP during the snowfall season, and it decreased to 67 and 64% during the snowmelt and rainfall seasons, respectively. These results indicate that PON and POP are important forms of nitrogen and phosphorous loss from the land that need to be quantified and understood. In this study, a significant linear relationship was found between PON, POP and sediment concentration (Fig. 2). It indicates that PON and POP were mainly transported with suspended sediment, because particulate nutrient losses from land to rivers were mainly caused by land surface soil erosion. However, the data are quite scattered to the regression line, it is because that there are spatially varied sources of sediment and associated particulate nutrients from different land uses and soil types in the study site.

Hydrology

Table 1 presents the calibrated parameters for discharge, whereas Figure 3 graphically illustrates the comparison between the observed and simulated daily

Table 3. Optimum values of sediment parameters in SWAT.

No.	Parameter	Definition of parameters	Fitted value
1	USLE_C(FRST).crop.dat	Minimum value for the cover and management factor for the land cover	0.02
2	USLE_C(PAST).crop.dat	Minimum value for the cover and management factor for the land cover	0.03
3	USLE_P(FRST).mgt	USLE support practice factor	0.9
4	USLE_P(PAST).mgt	USLE support practice factor	0.85
5	CH_EROD.rte	Channel erodibility factor	0.01
6	CH_COV.rte	Channel cover factor	1
7	PRF.bsn	Peak rate adjustment factor in the main channel	0.56
8	SPCON.bsn	Coefficient in sediment transport equation	0.01
9	SPEXP.bsn	Exponent in sediment transport equation	2

Table 4. Partition of dissolved and particulate nitrogen and phosphorous for snowfall, snowmelt and rainfall seasons during 2003, 2004 and 2007.

Hydrological events		TN ($mg.L^{-1}$)	TDN ($mg.L^{-1}$)	PON ($mg.L^{-1}$)	TP ($mg.L^{-1}$)	TDP ($mg.L^{-1}$)	POP ($mg.L^{-1}$)
Snowfall season (Dec–Mar) $N = 17$	Average	1.042	1.004	0.039	0.028	0.002	0.026
	Percentage		96%	4%		8%	92%
Snowmelt season (Apr–May) $N = 139$	Average	1.264	0.972	0.292	0.058	0.019	0.039
	Percentage		77%	23%		33%	67%
Rainfall season (Jun–Nov) $N = 431$	Average	1.349	0.916	0.433	0.083	0.030	0.054
	Percentage		68%	32%		36%	64%

TN, total nitrogen; TDN, total dissolved nitrogen; PON, particulate organic nitrogen; TP, total phosphorous; TDP, total dissolved phosphorous; POP, particulate organic phosphorous.

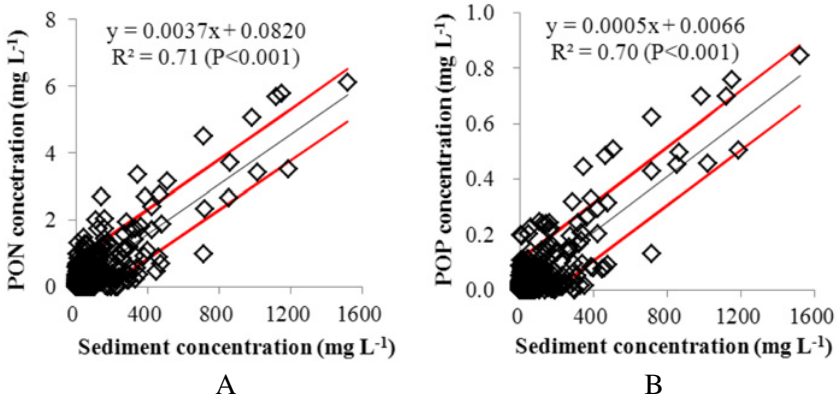

Fig. 2. Relationships between measured instantaneous sediment and (A) particulate organic nitrogen (PON), and (B) particulate organic phosphorous (POP) concentration. Red line shows 95% prediction interval.

discharge at the main outlet of the SRW. The simulated discharge followed a similar trend to the observed discharge. The statistical performance of the SWAT for daily streamflow estimation was satisfactory (calibration period: $R^2 = 0.60$, $E_{NS} = 0.40$ and $Re = 14\%$; validation period: $R^2 = 0.87$, $E_{NS} = 0.61$ and $Re = 7\%$). The SWAT model yielded a mean annual streamflow of 1140 mm for the period studied (2003–2008), which was close to the observed value of 1054 mm. However, the simulated peak discharge was underestimated during some heavy rainfall periods such as events in August 2003 and October 2006. This was primarily due to the surface runoff was underestimated for these events in this study. It might be because precipitation duration and intensity are not being considered by the soil conservation services (SCS) curve number (CN) method (SCS, 1972) for simulation of streamflow in SWAT model as reported by Phomcha *et al.* (2011). This limitation might be more profound for the heavy rainfall events.

Mean annual rainfall for the total simulation period (2003–2008) over the area of the catchment was 1055 mm. Simulated results showed that about 430 mm (41%) was removed through evapotranspiration (ET). Simulated mean annual water yield was 1140 mm, including surface runoff of 30 mm (2.5%), lateral flow of 145 mm (13%) and groundwater recharge of 965 mm (84.5%), including EXT of 480 mm (42%). In the SRW, most stream water was recharged by subsurface flow throughout the year. The computed water balance components indicated low surface runoff (2.5% of total water yield) that subsequently caused landscape erosion. Since the watershed studied is characterized by volcanogeneous soils with high hydraulic conductivities (Table 2) and porosities, surface runoff due to infiltration excess is probably of little importance

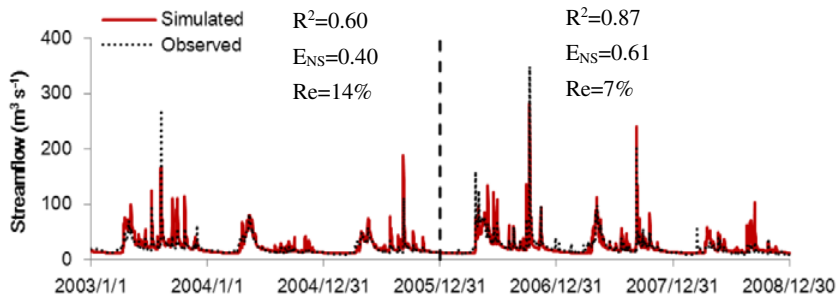

Fig. 3. Daily stream flow calibration and validation for the Shibetsu River watershed performed with the SWAT model (2003–2008). Grey dash line separates the calibration and validation periods.

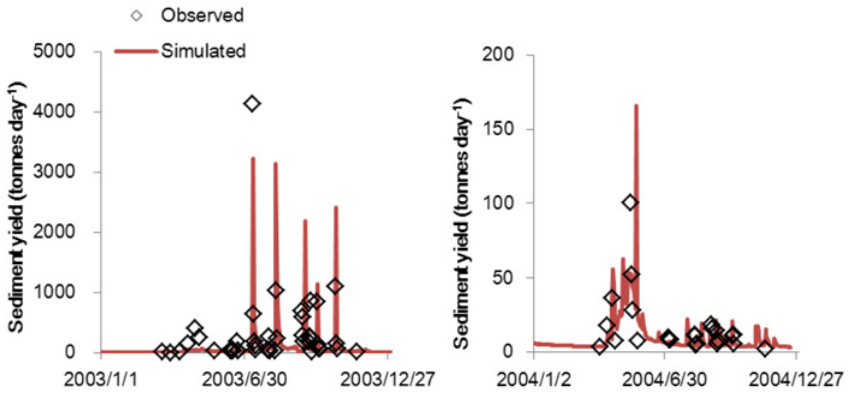

Fig. 4. Comparison between observed daily sediment yield and simulated values obtained by the SWAT model (2003–2004).

and dominating flow processes are likely to happen in the subsurface (Blume, 2008). The large subsurface storage can retain most of the incident rainfall during events (> 90%, often even > 95%) as reported by Blume (2008).

Modelling performance of SWAT for sediment yield estimation

Table 3 presents the calibrated parameters for sediment yield simulation. The SWAT model performance statistics are shown in Table 5. Figure 4 generally indicates that the simulated daily sediment loads of the SWAT model and the observed values are comparable, yielding R^2 of 0.62, E_{NS} of 0.48 and Re of 10% in the calibration period, and R^2 of 0.64, E_{NS} of 0.61 and Re of 14% in the validation period (Table 5). Overall, the SWAT model was able to simulate sediment yield with reasonable accuracy on a daily time step. Simulated annual sediment yield from 2003 to 2008 ranged from 5 to 45 tonnes.km^{-2}.yr^{-1} (annual mean of 24 tonnes.km^{-2}.yr^{-1}) (Fig. 5(A)). The SWAT model predicted acceptable model performance with a short time step (daily), indicating that this model can be considered an appropriate tool for estimating sediment yield in the SRW.

The snowfall, snowmelt and rainfall seasons contributed around 10, 20 and 70% respectively to total sediment and associated PON and POP yields. Rainfall season play an important role in sediment transport, as most

Table 5. Performance of the SWAT model for estimating daily sediment and particulate organic nitrogen (PON) and particulate organic phosphorous (POP) yields.

Model performance	Sediment 2003	Sediment 2004	PON 2003–2004	POP 2003–2004
R^2	0.62	0.64	0.65	0.70
E_{NS}	0.48	0.61	0.65	0.70
Re (%)	10	14	1	7

of the annual sediment yield from a watershed can be transported by a stream during a small number of rainfall events that occur in a relatively short period of time within a year. However, a comparison of the results indicates that the SWAT model might overestimate the sediment load for some high-flow events (Fig. 4) because the SWAT model allows all the soil eroded by runoff to reach the river directly, without considering sediment deposition remaining on surface catchment areas. The results also indicate that the SWAT model underestimated the sediment load of some peak events (Fig. 4). This might be because the sediment routing algorithm used in SWAT is very simplified. The topographic factor (LS_{USLE}) automatically estimated from the DEM in the SWAT model was found to contain errors (Kim *et al.*, 2009; Babel *et al.*, 2011), it partially explains the model inaccuracies for sediment yield estimation. With better accuracy and resolution of DEM and more reliable methods for derivation of the topographical variables related to LS_{USLE}, such as slope

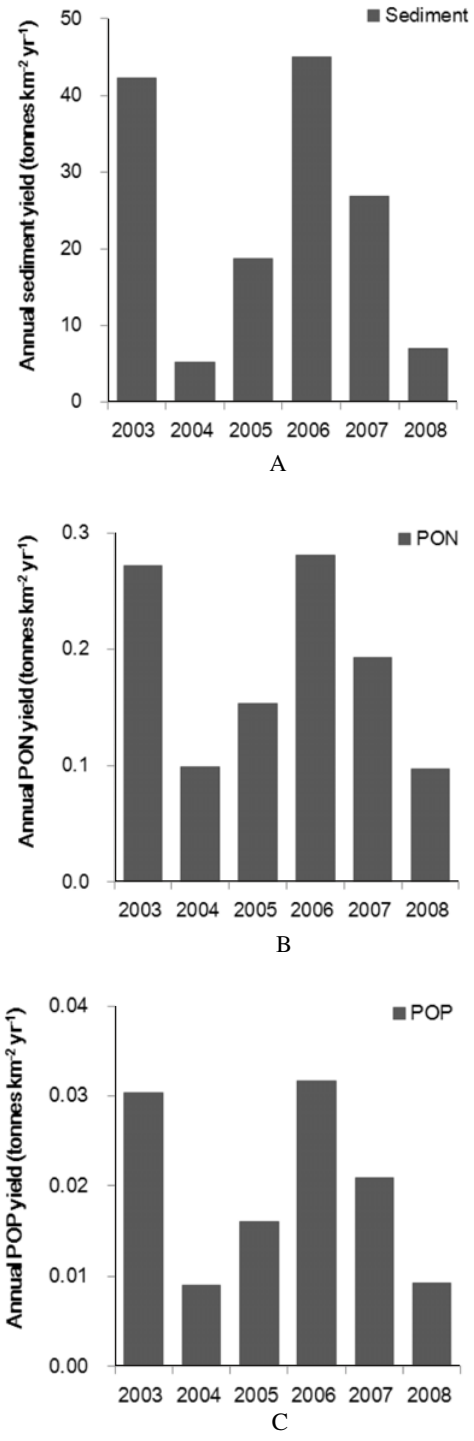

Fig. 5. Simulated annual sediment (A), particulate organic nitrogen (PON) (B) and particulate organic phosphorous (POP) (C) yields (2003–2008).

length and steepness, it would be possible to enhance precision of the model (Van Remortel *et al.*, 2001). The land cover and management factor (USLE_C) was classified and assigned corresponding values in the SWAT model (Table 3). This method, however, results in USLE_C factor that is homogeneous for each HRU which might cover relatively large areas and do not adequately reflect spatial variations in vegetation density within cover classes or over large geographic areas (Wang *et al.*, 2002; Yang, 2014). Determining USLE_C factor value as a function of fractional bare soil and vegetation cover could be implemented in SWAT model to improve sediment predictions (Benkobi *et al.*, 1994; Yang, 2014). The MUSLE method improves upon the USLE and RUSLE methods by explicitly considering runoff (Kinnell, 2005). However, Qiu *et al.* (2012) pointed out that the SWAT model sediment predication error most likely resulted from the limitations of the existing the SCS-CN method and MUSLE method. The studied watershed had intense rainfall and heavy storm events with high potential to erode surface soil, but the SCS-CN and MUSLE do not account for detailed characteristics of rainfall as reported by Phomcha *et al.* (2011). Modification of SWAT components may be needed to take rainfall intensity and its duration into account to enhance the model performance on peak flow and sediment load simulation during the heavy rainfall season.

Estimation of PON and POP yields with SWAT

Statistically significant relationships were found between PON and POP concentration and sediment concentration (Fig. 2). Linear relationships between sediment and particulate nutrients have also been found by other researchers (Kronvang *et al.*, 1997; Oeurng *et al.*, 2011). Based on these relationships, temporal variation in PON and POP yields could be computed from the simulated daily sediment yield obtained from the SWAT model (Fig. 4). The daily PON and POP yields showed a strong variability due to the variability in sediment yield within the catchment. Figure 6 shows that simulated daily PON and POP yields are comparable with the observed results during 2003–2004, which yielded R^2 of 0.65, E_{NS} of 0.65 and Re of 1% for PON yield, and R^2 of 0.70, E_{NS} of 0.70 and Re of 7% for POP yield (Table 5). Simulated annual PON and POP yields from 2003 to 2008 showed that the annual PON yield ranged from 0.1 to 0.3 tonnes.km^{-2}.yr^{-1} (annual mean of 0.18 tonnes.km^{-2}.yr^{-1}; Fig. 5(B)), and annual POP yield ranged from 0.01 to 0.03 tonnes.km^{-2}.yr^{-1} (annual mean of 0.02 tonnes.km^{-2}.yr^{-1}; Fig. 5(C)) at the main outlet of the SRW. Appropriate strategies should be advised to protect critical areas with high soil erosion that also are the critical source area for PON and POP exports.

Identification of critical source areas of land surface erosion

During the studied years (2003–2008), SWAT model simulation results showed that sediment delivery ratio in each channel was close to one, it indicates that in-stream erosion/sedimentation might be of little importance in SRW. The average annual sediment contribution from the individual sub-basin was investigated to determine its relative source contribution with the SWAT

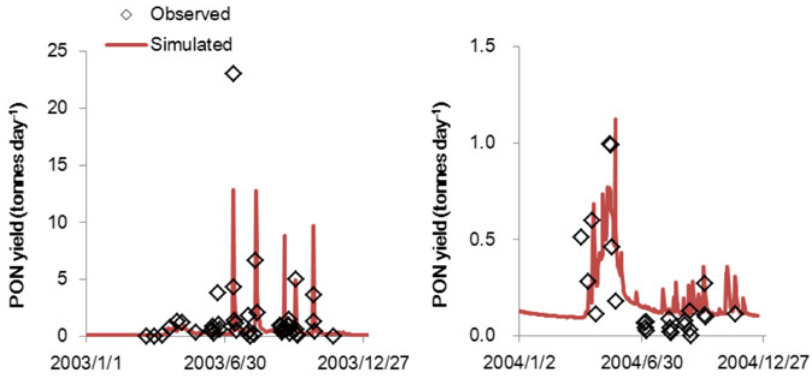

A

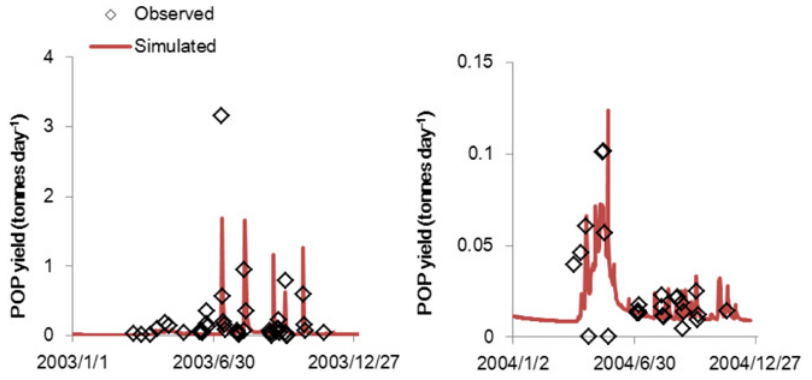

B

Fig. 6. Comparison between simulated and observed daily particulate organic nitrogen (PON) (A) and particulate organic phosphorous (POP) (B) yields (2003–2004).

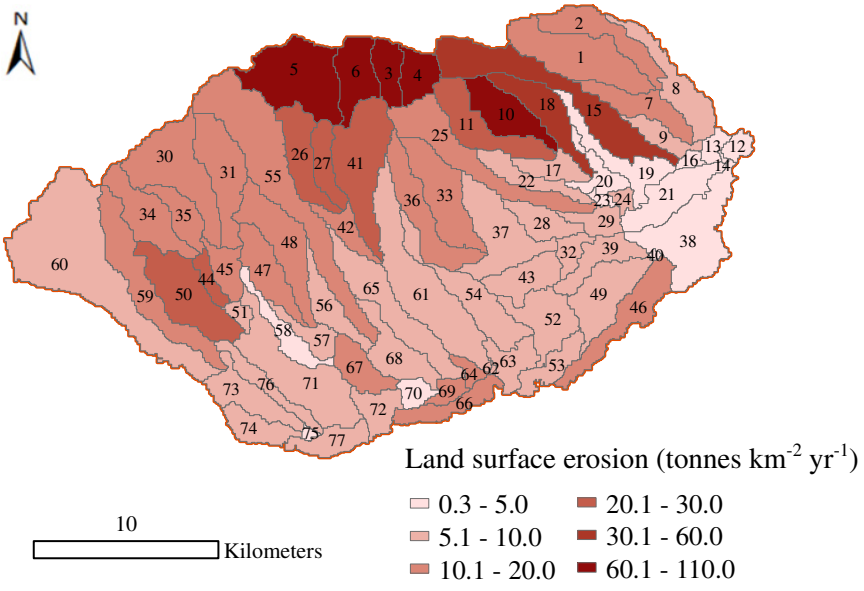

Fig. 7. Average annual land surface erosion. Numbers show locations of the sub-basins in the watershed.

model. With the current fitted parameters (Tables 2 and 3), results showed that sub-basins 3, 4, 5, 6 and 10 in the forest area had the highest sediment yield (60.1–110.0 tonnes.km^{-2}.yr^{-1}) compared to the neighbouring sub-basins (Fig. 7). The sediment yield value was similar to the results reported by Saghafian *et al.* (2012). These sub-basins with the highest elevation and slopes greater than 10° were identified as the most critical source areas of land

surface erosion, even though they are covered by forest (Fig. 1). Other sub-basins in the forest area with steep slopes above 10° were also found to have a relatively high sediment contribution (20.1–60.0 tonnes.km^{-2}.yr^{-1}). Under agricultural pastureland, sediment yield increased with the distance from the watershed outlet. For example, the sediment contribution was higher in sub-basins 46, near 66 and 67 due to a small proportion of steep slopes in this area (Fig. 7). Topography had an influence in that sub-basins further from the outlet had a relatively high elevation and featured slopes under agricultural pastureland. Soil erosion increased with steepness of the slope, which is most likely the reason for a higher sediment yield in these sub-basins (Wu and Chen, 2012). Results from this study indicated that topography might play an important role in land surface erosion. Agricultural land use with a small proportion of steep slopes can be a critical sediment source area, even though flat terrain is found in most areas. Best management practices for effective anti-erosion, such as reduced tillage, contour cropping, the establishment of buffer strips and riparian zones, and the construction of settling ponds and wetlands, could be important in preventing soil detachment and transport from cultivated fields (Boardman *et al.*, 2009; Ekholm and Lehtoranta, 2012). Riparian forests have been reported to play a function in soil conservation by sequestering hillslope-derived sediments at the watershed scale (Jolley *et al.*, 2010). In the present study site of the SRW, about 7 to 9% of land use consists of riparian forests, which would lead to the uncertainty in model simulation of land surface erosion because the soil conservation function of riparian forests was not considered during the simulation. Results from this study indicated that forest and pasture covers were not sufficient to protect slopes from soil erosion. Watershed managers should pay attention to areas with steep slopes when implementing best management practices to reduce non-point source pollution in the SRW from land surface erosion.

Summary and conclusions

Sediment and PON and POP yields were investigated in the SRW in Hokkaido (Japan), which is characterized by agricultural land use and forest, dominated by volcanic soils and recognized as the recipient of external groundwater.

The SWAT model, which includes the EXT contribution from HRUs to channels, was successfully used to quantify sediment and PON and POP yields at the main outlet of the SRW. Subbasins located in the upper part of the watershed were identified as critical source areas of land surface erosion. Effective anti-erosion management practices should be introduced here. The SWAT model could be used as an appropriate tool for estimating sediment and PON and POP yields and understanding soil erosion mechanisms in the SRW. However, a simplified hypothesis of EXT (1.38 mm.d^{-1}) was used in this study. More field work is required to shed light on spatial and temporal variations in EXT. More time and effort are also required to set up and calibrate the SWAT model with spatially distributed and temporally varied EXT for different HRUs in future.

Acknowledgements. This study was commissioned by the Japan Atomic Energy Agency, as part of project FY2013.

References

Abbaspour K.C., 2007. User Manual for SWAT-CUP, SWAT Calibration and Uncertainty Analysis Programs, Swiss Federal Institute of Aquatic Science and Technology, Eawag, Duebendorf, Switzerland, 103 p.

Arnold J.G., Moriasi D.N., Gassman P.W., Abbaspour K.C., White M.J., Srinivasan R. and Jha M.K., 2012. SWAT: model use, calibration, and validation. *Trans. ASABE*, *55*, 1491–1508.

Babel M.S., Shrestha B. and Perret S., 2011. Hydrological impact of biofuel production: a case study of the Khlong Phlo Watershed in Thailand. *Agric. Water Manage.*, *101*, 8–26.

Bagnold R.A., 1977. Bed load transport by natural rivers. *Water Resour. Res.*, *13*, 303–312.

Benkobi L., Trlica M.J. and Smith J.L., 1994. Evaluation of a refined surface cover subfactor for use in RUSLE. *J. Range Manage.*, *47*, 74–78.

Blume T., 2008. Hydrological processes in volcanic ash soils – measuring, modeling and understanding runoff generation in an undisturbed catchment. PhD thesis, Faculty of Mathematics and Natural Sciences, University of Potsdam, Germany, 153 p.

Boardman J., Shepheard M.L., Walker E. and Foster I.D.L., 2009. Soil erosion and risk-assessment for on- and off-farm impacts: a test case using the Midhurst area, West Sussex, UK. *J. Environ. Manage.*, *90*, 2578–2588.

Boithias L., Sauvage S., Taghavi L., Merlina G., Probst J.L. and Sánchez-Pérez J.M., 2011. Occurrence of metolachlor and trifluralin losses in the Save River agricultural catchment during floods. *J. Hazard. Mater.*, *196*, 210–219.

Boithias L., Srinivasan R., Sauvage S., Macary F. and Sánchez-Pérez J.M., 2013. Daily nitrate losses: implication on long-term river quality in an intensive agricultural catchment (south-western France). *J. Environ. Qual.*, *43*, 46–54.

Cerro I., Sánchez-Pérez J.M., Ruiz-Romera E. and Antigüedad I., 2013. Variability of particulate (SS, POC) and dissolved (DOC, NO_3) matter during storm events in the Alegria agricultural watershed. *Hydrol. Process.*, *28*, 2855–2867.

Cerro I., Antigüedad I., Srinivasan R., Sauvage S., Volk M. and Sánchez-Pérez J.M., 2014. Simulating land management options to reduce nitrate pollution in an agricultural watershed dominated by an alluvial aquifer. *J. Environ. Qual.*, *43*, 67–74.

Chu T.W., Shirmohammadi A., Montas H. and Sadeghi A., 2004. Evaluation of the SWAT model's sediment and nutrient components in the Piedmont physiographic region of Maryland. *Trans. ASAE*, *47*, 1523–1538.

Cultivated Soil Classification committee, Japan, 1995. Classification of Cultivated Soil in Japan, Third

Approximation, Miscellaneous Publication, National Institute for Agro-Environmental Sciences, 17, Tsukuba, 79 p.

Easton Z.M., Fuka D.R., White E.D., Collick A.S., Biruk Ashagre B., McCartney M., Awulachew S.B., Ahmed A.A. and Steenhuis T.S., 2010. A multi basin SWAT model analysis of runoff and sedimentation in the Blue Nile, Ethiopia, Hydrol. *Earth Syst. Sci.*, *14*, 1827–1841.

Ekholm P. and Lehtoranta J., 2012. Does control of soil erosion inhibit aquatic eutrophication? *J. Environ. Manage.*, *93*, 140–146.

Gao P., 2008. Understanding watershed suspended sediment transport. *Prog. Phys. Geog.*, *32*, 243–263.

Haag I., Kern U. and Westrich B., 2001. Erosion investigation and sediment quality measurements for a comprehensive risk assessment of contaminated aquatic sediments. *Sci. Total Environ.*, *266*, 249–257.

Hayakawa A., Woli K.P., Shimizu M., Nomaru K., Kuramochi K. and Hatano R., 2009. The nitrogen budget and relationships with riverine nitrogen exports of a dairy cattle farming catchment in eastern Hokkaido, Japan. *Soil Sci. Plant Nutr.*, *55*, 800–819.

Heathwaite A.L., Dils R.M., Liu S., Carvalho L., Brazier R.E., Pope L., Hughes M., Philips G. and May L., 2005. A tiered risk-based approach for predicting diffuse and point source phosphorus losses in agricultural areas. *Sci. Total Environ.*, *344*, 225–239.

IUSS, ISRIC, FAO, 2006. World Reference Base for Soil Resources. World Soil Resources Reports 103. International Union of Soil Sciences, ISRIC World Soil Information, FAO, Rome, 128 p.

Jayakrishnan R., Srinivasan R., Santhi C. and Arnold J.G., 2005. Advances in the application of the SWAT model for water resources management. *Hydrol. Process.*, *19*, 749–762.

Jiang R., Li Y., Wang Q., Kuramochi K., Hayakawa A., Woli K.P. and Hatano R., 2011. Modeling the water balance processes for understanding the components of river discharge in a non-conservative watershed. *Trans. ASABE*, *54*, 2171–2180.

Jiang R., Wang C.Y., Hatano R., Hayakawa A., Woli K.P. and Kuramochi K., 2014. Simulation of stream nitrate-nitrogen export using the Soil and Water Assessment Tool model in a dairy farming watershed with an external water source. *J. Soil Water Conserv.*, *69*, 75–85.

Jolley R.L., Lockaby B.G. and Cavalcanti G.G., 2010. Changes in riparian forest composition along a sedimentation rate gradient. *Plant Ecol.*, *210*, 317–330.

Kerr J.G., Burford M.A., Olley J.M., Bunn S.E. and Udy J., 2011. Examining the link between terrestrial and aquatic phosphorus speciation in a subtropical catchment: the role of selective erosion and transport of fine sediments during storm events. *Water Res.*, *45*, 3331–3340.

Kim J.G., Park Y.S., Yoo D., Kim N., Engel B.A., Kim S., Kim K.S. and Lim K.J., 2009. Development of a SWAT patch for better estimation of sediment yield in steep sloping watersheds. *J. Am. Water Resour. Assoc.*, *45*, 963–972.

Kinnell P.I.A., 2005. Why the universal soil loss equation and the revised version of it do not predict event erosion well. *Hydrol. Process.*, *19*, 851–854.

Kronvang B., Laubel A. and Grant R., 1997. Suspended sediment and particulate phosphorus transport and delivery pathways in an arable catchment, Gelbaek stream, Denmark. *Hydrol. Process.*, *11*, 627–642.

Lal R., 1998. Soil erosion impact on agronomic productivity and environment quality. *Crit. Rev. Plant Sci.*, *17*, 319–464.

Le Moine N., Andréassian V., Perrin C. and Michel C., 2007. How can rainfall-runoff models handle intercatchment groundwater flows? Theoretical study based on 1040 French catchments. *Water Resour. Res.*, *43*, W06428.

Le Moine N., Andréassian V. and Mathevet T., 2008. Confronting surface and groundwater balances on the La Rochefoucauld-Touvre karstic system (Charente, France). *Water Resour. Res.*, *44*, W03403.

Morgan R.P.C., Quinton J.N., Smith R.E., Govers G., Poesen J.W.A., Auerswald K., Chisci G., Torri D. and Styczen M.E., 1998. The European soil erosion model (EUROSEM): a dynamic approach for predicting sediment transport from fields and small catchments. *Earth Surf. Proc. Land.*, *23*, 527–544.

Mukundan R., Radcliffe D.E. and Risse L.M., 2010. Spatial resolution of soil data and channel erosion effects on SWAT model predictions of flow and sediment. *J. Soil Water Conserv.*, *65*, 92–104.

Nash J.E. and Sutcliffe J.V., 1970. River flow forecasting through conceptual models. Part 1: a discussion of principles. *J. Hydrol.*, *10*, 282–290.

Nearing M.A., Foster G.R., Lane L.J. and Finkner S.C., 1989. A process-based soil erosion model for USD-Water Erosion Prediction Project Technology. *Trans. ASAE*, *32*, 1587–1593.

Neitsch S.L., Arnold J.G., Kiniry J.R., Williams J.R. and King K.W., 2005. Soil and Water Assessment Tool. Theoretical Documentation: Version 2005. TWRI TR–191. Texas Water Resources Institute, College Station, Texas, 476 p.

Oeurng C., Sauvage S. and Sánchez-Pérez J.M., 2011. Assessment of hydrology, sediment and particulate organic carbon yield in a large agricultural catchment using the SWAT model. *J. Hydrol.*, *401*, 145–153.

Phomcha P., Wirojanagud P., Vangpaisal T. and Thaveevouthti T., 2011. Predicting sediment discharge in an agricultural watershed: a case study of the Lam Sonthi watershed, Thailand. *Science Asia*, *37*, 43–50.

Qiu L.J., Zheng F.L. and Yin R.S., 2012. SWAT-based runoff and sediment simulation in a small watershed, the loessial hilly-gullied region of China: capabilities and challenges. *Int. J. Sediment Res.*, *27*, 226–234.

Saghafian B., Sima S., Sadeghi C. and Jeirani F., 2012. Application of unit response approach for spatial prioritization of runoff and sediment sources. *Agric. Water Manage.*, *109*, 36–45.

Salerno F. and Tartari G., 2009. A coupled approach of surface hydrological modelling and wavelet analysis for understanding the baseflow components of river discharge in karst environments. *J. Hydrol.*, *376*, 295–306.

Santhi C., Arnold J.G., Williams J.R., Dugas W.A., Srinivasan R. and Hauck L.M., 2001. Validation of the SWAT model on a large river basin with point and nonpoint sources. *J. Am. Water Resour. Assoc.*, *37*, 1169–1188.

SCS (Soil Conservation Service), 1972. Section 4: Hydrology in National Engineering Handbook, U.S. Department of Agriculture-Soil Conservation Service, Washington, D.C., 55 p.

Talebizadeh M., Morid S., Ayyoubzadeh S.A. and Ghasemzadeh M., 2010. Uncertainty analysis in sediment load modeling using ANN and SWAT model. *Water Resour. Manage.*, *24*, 1747–1761.

Thomas R.B., 1988. Monitoring baseline suspended sediment in forested basin: the effect of sampling on suspended sediment rating curves. *Hydrol. Sci. J.*, *33*, 499–514.

Van Remortel R.D., Hamilton M.E. and Hickey R.J., 2001. Estimating the LS factor for RUSLE through iterative slope length processing of digital elevation data within Arclnfo grid. *Cartography*, *30*, 27–35.

Van Rompaey A.J.J., Verstraeten G., Van Oost K., Govers G. and Poesen J., 2001. Modelling mean annual sediment yield using a distributed approach. *Earth Surf. Proc. Land.*, *2*, 1221–1236.

Wang G.S., Wente G. and Anderson A., 2002. Improvement in mapping vegetation cover factor for the universal soil loss equation by geostatistical methods with Landsat Thematic Mapper images. *Int. J. Remote Sens.*, *23*, 3649–3667.

Williams J.R., 1975. Sediment routing for agricultural watersheds. *J. Am. Water Resour. Assoc.*, *11*, 965–974.

Williams J.R., 1995. The EPIC model. *In*: Singh V.P. (ed.), Computer Models of Watershed Hydrology, Water Resources Publications, Highlands Ranch, CO, 909–1000.

Woli K.P., Nagumo T., Kuramochi K. and Hatano R., 2004. Evaluating river water quality through land use analysis and N budget approaches in livestock farming areas. *Sci. Total Environ.*, *329*, 61–74.

Wu Y. and Chen J., 2012. Modeling of soil erosion and sediment transport in the East River Basin in southern China. *Sci. Total Environ.*, *441*, 159–168.

Yang X., 2014. Deriving RUSLE cover factor from time-series fractional vegetation cover for hillslope erosion modelling in New South Wales. *Soil Res.*, *52*, 253–261.